

## Can a C–H···O Interaction Be a Determinant of Conformation?

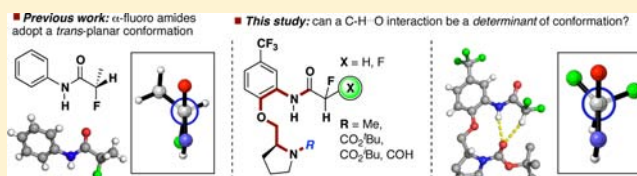
Christopher R. Jones,<sup>†</sup> Pranjal K. Baruah,<sup>†</sup> Amber L. Thompson,<sup>†</sup> Steve Scheiner,<sup>\*,‡</sup> and Martin D. Smith<sup>\*,†</sup>

<sup>†</sup>Chemistry Research Laboratory, University of Oxford, 12 Mansfield Road, Oxford OX1 3TA, U.K.

<sup>‡</sup>Department of Chemistry & Biochemistry, Utah State University, Logan, Utah 84322-0300, United States

### Supporting Information

**ABSTRACT:** Whether nonconventional hydrogen bonds, such as the C–H···O interaction, are a consequence or a determinant of conformation is a long-running and unresolved issue. Here we outline a solid-state and quantum mechanical study designed to investigate whether a C–H···O interaction can override the significant *trans*-planar conformational preferences of  $\alpha$ -fluoroamide substituents. A profound change in dihedral angle from *trans*-planar<sub>(OCCF)</sub> to *cis*-planar<sub>(OCCF)</sub> observed on introducing an acceptor group for a C–H···O hydrogen bond is consistent with this interaction functioning as a determinant of conformation in certain systems. This testifies to the potential influence of the C–H···O hydrogen bond and is consistent with the assignment of this interaction as a contributor to overall conformation in both model and natural systems.



## INTRODUCTION

Conventional hydrogen bonds between main-chain amide and carbonyl groups are significant contributors to the structural and catalytic functions of proteins, but less electronegative atoms such as carbon are often observed in close proximity to acceptor atoms such as oxygen.<sup>1–6</sup> Challenges in elucidating the difference between a coincidental contact (where the two groups happen to lie close together as a consequence of the structure of the entire molecule) from an attractive C–H···O contact<sup>7</sup> have led to significant discussion over the true nature of these interactions.<sup>8–12</sup> For example, a short C–H···O contact in bacteriorhodopsin has been demonstrated to be nonstabilizing,<sup>13,14</sup> while it has been reported that the X-ray crystal structure of a hydrated tricyclic orthoamide possessed an eclipsed C(sp<sup>3</sup>)–CH<sub>3</sub> group as a consequence of three C–H···O interactions.<sup>15,16</sup> The C–H···O interaction has also been proposed to have a significant influence on the transition states of certain catalytic asymmetric transformations.<sup>17,18</sup> This emphasizes that the context of these interactions is important in determining their contribution to an overall structural picture. Solid-state studies of crystals provide a wealth of information about small-molecule geometry but betray little about the energetic aspects of noncovalent interactions, and hence we reasoned that a combined X-ray study and theoretical analysis of an unnatural model system could provide insight into the potential strength and conformational influence of this interaction.<sup>19</sup>

**Study Design.** We have previously demonstrated that a prolinol–aromatic amine conjugate (Figure 1A) functions as a robust hydrogen-bonded parallel turn linker in the solid phase and in solution,<sup>20,21</sup> and we decided to exploit this template in the design of a test-bed to investigate the conformational influence that a C–H···O interaction may impose. We

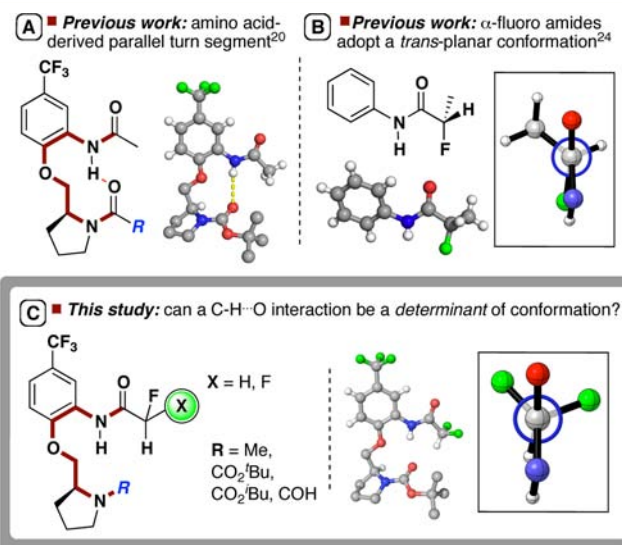


**Figure 1.** Previous work and outline of current study.

rationalized that substituting the  $\alpha$ -position of the amide in this turn motif with electron-withdrawing groups such as fluorine<sup>22</sup> would increase the acidity of the  $\alpha$ -C–H proton, with a concomitant increase in the hydrogen bond donor ability of this group.<sup>23</sup>

Work from O'Hagan and co-workers has demonstrated that  $\alpha$ -fluoroamides adopt a *trans*-planar conformation in the solid state, with a deep potential minimum of ca. 7 kcal mol<sup>–1</sup>, predominantly as a consequence of an interaction between the

Received: February 23, 2012

Published: July 12, 2012

fluorine lone pairs and the N–H  $\sigma^*$  orbital (Figure 1B).<sup>24,25</sup> Exploring turn segments functionalized with  $\alpha$ -fluoroamides<sup>26,27</sup> would offer an opportunity to investigate whether the C–H $\cdots$ O interaction can function as a determinant of conformation<sup>28</sup> by overriding the inherent rotational preferences of the fluoroamide substituent (Figure 1C).<sup>29–32</sup> In this paper, we describe the solid-state structures of a series of  $\alpha$ -fluoroamides based around a parallel-turn structure and, through quantum mechanical calculations, deconstruct the contributions that each noncovalent interaction has on the rotational preferences of the fluoroamide group to show that in certain circumstances the C–H $\cdots$ O interaction functions as a determinant of conformation.

## RESULTS AND DISCUSSION

**1. Model Calculations.** To extract the intrinsic rotational preferences of the fluoroamide group, we focused on 2-fluoro-N-methylacetamide as a model system. Calculations were performed at the B3LYP level with a 6-31+G\*\* basis set, which contains polarization functions on all atoms and diffuse functions on the non-hydrogen atoms, thereby offering a balanced representation of electronic effects. For a series of dihedral  $\varphi_{(\text{OCCF})}$  angles, the geometry was fully optimized, tracing out a rotational profile (Figure 2A) that shows a clear minimum when the oxygen and fluorine atoms are opposite one another ( $\varphi_{(\text{OCCF})} = 180^\circ$ ), consistent with that reported by O'Hagan.<sup>24,33</sup>

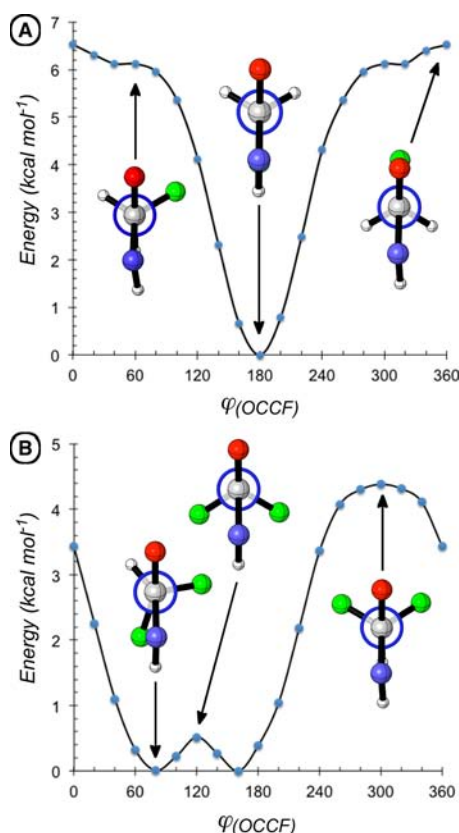


**Figure 2.** Computed rotational profiles of model fluoroamides (a)  $\text{CH}_3\text{NHCOCH}_2\text{F}$  and (b)  $\text{CH}_3\text{NHCOCHF}_2$  as a function of dihedral angle  $\varphi_{(\text{OCCF})}$ . Optimized structures are illustrated for some of the more important geometries.

Rotation of the  $\text{CH}_2\text{F}$  group away from this position raises the energy of the system, and a maximum is reached when the oxygen and fluorine atom are *syn* ( $\varphi_{(\text{OCCF})} = 0^\circ$ ), about  $6.5 \text{ kcal mol}^{-1}$  higher in energy than the minimum. There is a shoulder in the profile at a dihedral angle of  $60^\circ$ , when the  $\text{CH}_2\text{F}$  group is staggered relative to the oxygen. In order to ensure that these results are not a product of a specific theoretical method, the structures were reoptimized at the MP2 level with the 6-31+G\*\* basis set. The relative energies were essentially unchanged, within  $0.1 \text{ kcal mol}^{-1}$ . A considerably larger and more flexible aug-cc-pVTZ basis set was also applied at the MP2 level leading to some small changes including a flattening of the barrier to rotation in the monofluoro substituted case from  $6.5$  to  $5.8 \text{ kcal mol}^{-1}$ . When a second fluorine atom is added to the system (Figure 2B),<sup>34</sup> the highest energy structure, about  $4.5 \text{ kcal mol}^{-1}$  higher than the optimized geometry, is when both of these fluorine atoms are close to the oxygen, with dihedral angles  $\varphi_{(\text{OCCF})}$  of  $\pm 60^\circ$ , respectively. This structure is less stable than that in which one of the fluorine atoms eclipses the oxygen (with  $\varphi_{(\text{OCCF})} = 0^\circ$ ), and the other is moved further away to  $120^\circ$ . The optimized geometry occurs for  $\varphi_{(\text{OCCF})} = 161^\circ$  (and its symmetrical counterpart at  $59^\circ$ ), which is skewed by about  $20^\circ$  from the placement of one fluorine atom directly opposite the oxygen, probably as a consequence of the rotational preferences of the other fluorine. As such, the two  $\varphi_{(\text{OCCF})}$  dihedral angles of  $161^\circ$  and  $-82^\circ$  are preferable to  $180^\circ$  and  $-60^\circ$ , by about  $0.5 \text{ kcal mol}^{-1}$ . This is consistent with the reported orientation of a difluoroamide incorporated into a helical  $\beta$ -peptide where one fluorine is essentially antiperiplanar to the carbonyl group and the other *gauche*.<sup>35</sup>

**2. Solid-State Conformations.** We focused on the generation of a group of mono- and difluoroamide derivatives with a range of hydrogen bond acceptors. We rationalized that changing the size and electronic nature of the hydrogen bond acceptor could affect the propensity for the population of turn structures. With the intrinsic rotational preferences of monofluoro- and difluoroamide groups established through calculation, we examined their conformational preferences in the solid state using X-ray crystallography (Figure 3). 2-Fluoroacetamide, **1**, populates a conformation in the solid state<sup>33</sup> in which the C–F bond is *trans*-planar to the C=O with a dihedral angle of  $179^\circ$ , essentially identical to the theoretical model in Figure 2a; monofluoroamide **2**, lacking an intramolecular hydrogen bond acceptor, adopts a similar conformation, and both are consistent with the solid-state conformation described by O'Hagan<sup>24</sup> and with the theoretical model described earlier. In contrast, introducing a hydrogen-bond acceptor such as a *tert*-butyl carbamate (**3**, Figure 3C) leads to the population of a parallel turn-like structure and a profound conformational change to an orientation where the C–F bond is almost *cis*-planar to the C=O (with a dihedral angle of  $4(3)^\circ$ ), close to the calculated highest energy conformer in the model system (Figure 2A). It is also important to consider whether intermolecular interactions could affect the internal rotational states of the fluoroamide functionality. There are extensive intermolecular interactions in the structure of **1**, including N–H $\cdots$ O and C–H $\cdots$ O interactions. For control compound **2**, the aryl group appears to drive the crystal packing, with short  $\pi$ – $\pi$  contacts giving a layered structure.

The primary short contact in the solid state for **3** is an aryl C–H $\cdots$ F at  $3.14 \text{ \AA}$ , which leads to a herringbone-like motif; this

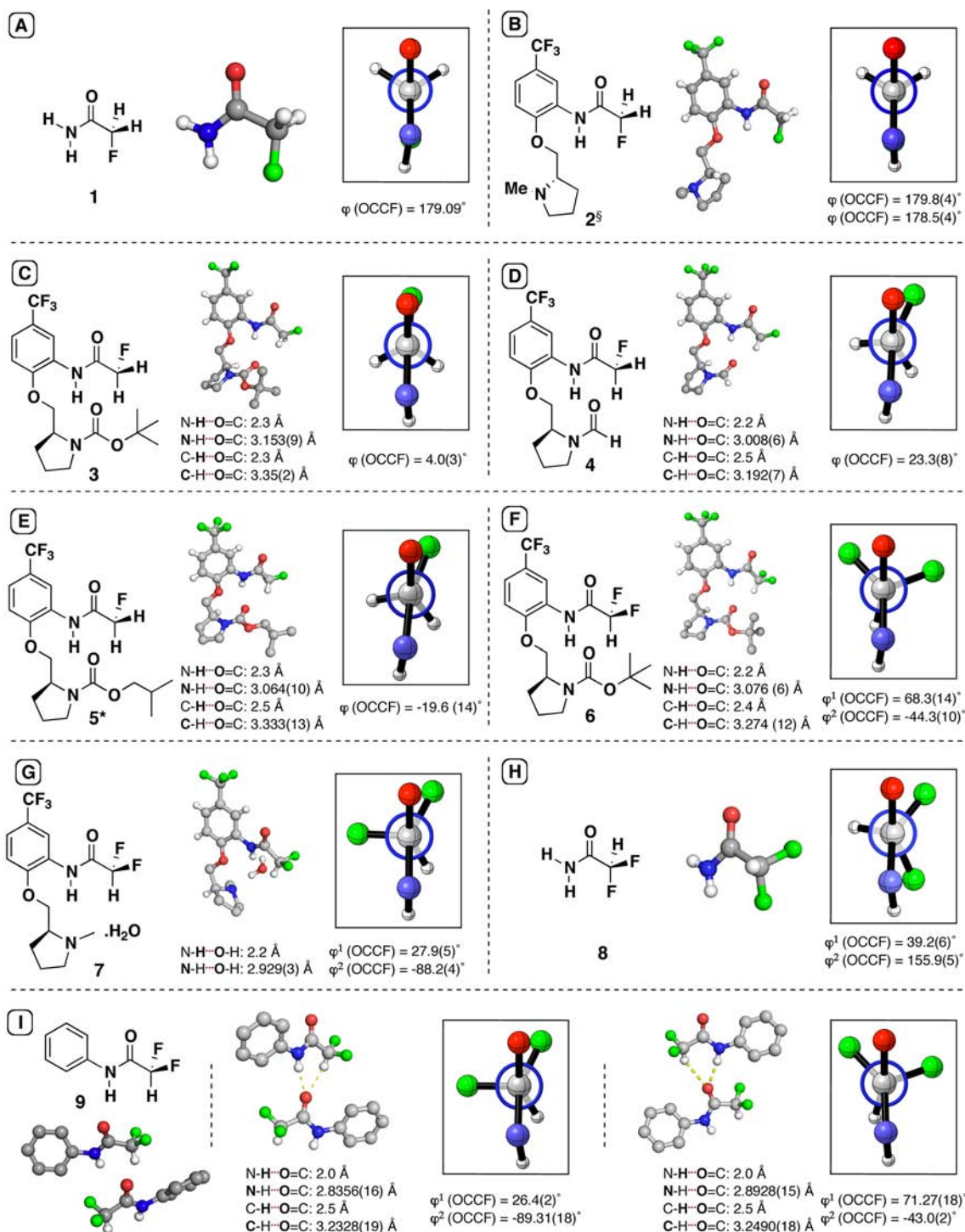


**Figure 3.** Solid-state conformations of monofluoro- and difluoroamides with relevant intramolecular distances (some atoms omitted for clarity). Variances, where available, are given in parentheses. Positions of hydrogen atoms are calculated. <sup>§</sup>Dihedral angles for both crystallographically unique molecules are given. \*Structure 5 has four crystallographically unique molecules and the fluoroamide groups in two are highly disordered; geometrical details are provided for one of the ordered molecules (although all populate a *cis*-planar arrangement).

is in the vicinity of disordered solvent, which suggests that the electrostatics in this area of the structure are not clearly defined. There is also a C–H...O contact, but as in **2**, there appears to be no obvious driving force for packing and the most obvious feature is the aromatic group that provides a nominally flat packing surface. Similar conformational effects are observed with different hydrogen bond acceptor groups: with a sterically

less demanding *N*-formyl group (**4**, Figure 3D), the dihedral angle is 23.3(8)°, and with an isobutyl group (Figure 3E), the dihedral angles are –19.6(14)° and –21.0(15)° for the ordered components. The presence of a hydrogen bond acceptor (as in Figure 3C–E) also leads to the amide NH approaching the carbonyl C=O at distances and geometry consistent with the presence of a hydrogen bond. A similarly dramatic effect is

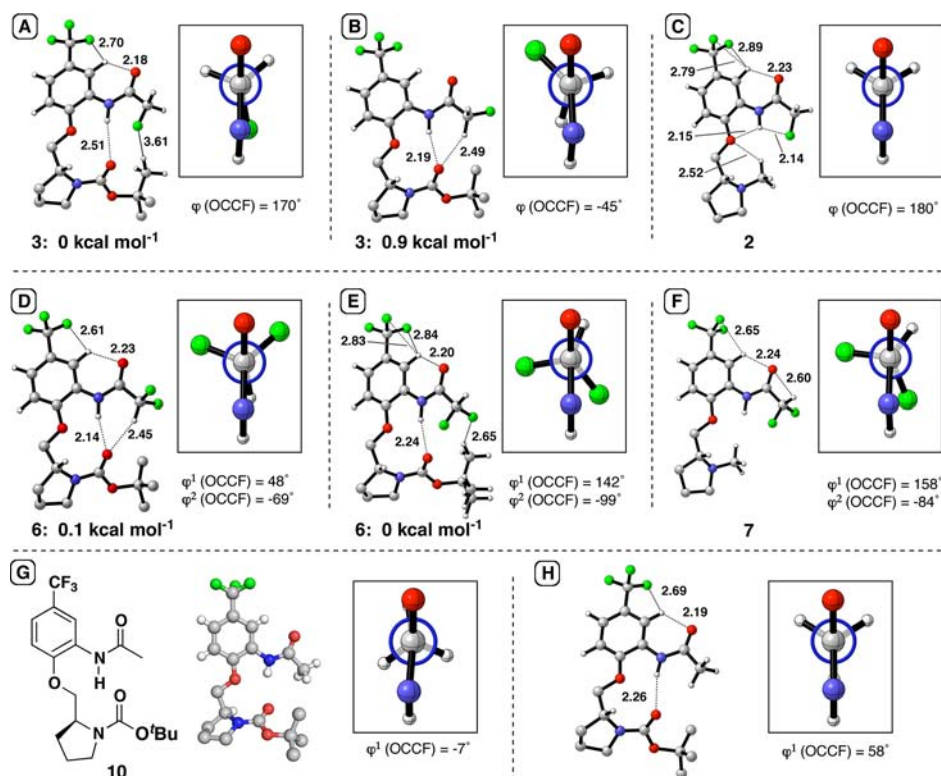


**Figure 4.** (A, B) Optimized geometries of two minima in the surface of **3**, (A)  $\varphi(\text{OCCF}) = 170^\circ$  and (B)  $\varphi(\text{OCCF}) = 215^\circ$ ; (C) optimized geometry of control molecule **2**; (D, E) optimized geometries of two minima of **6** in its surface, with  $\varphi(\text{OCCH}) = -168^\circ$  and  $20.5^\circ$ , respectively; (F) optimized geometry of control molecule **7** (some atoms omitted for clarity); distances are in Å; (G) X-ray structure of control compound **10**; (H) optimized geometry of control compound **10**.

observed in the difluoroamide system (Figure 3F). A turn-like structure is observed for **6**, the difluoro analogue of **3**, with internuclear N–H...O and C–H...O distances consistent with the presence of hydrogen bonds, and resultant dihedral angles  $\varphi(\text{OCCF})$  of  $68.3(14)^\circ$  and  $-44.3(10)^\circ$ , close to the maximum in the model rotational energy profile (Figure 2B). For **4**, there are more short intermolecular contacts, but these are primarily C–H...F involving the pyrrolidine ring. These involve the disordered component, suggesting that they are not a significant driving force for crystal packing. In the structure of **3**, there are also intermolecular C–H...O contacts as a consequence of the close proximity caused by efficient packing of the aromatic groups. Compound **5** is a structure with extensive disorder and pseudosymmetry, and unsurprisingly for a material that is so disordered, there are few meaningful short contacts. These involve the hydrogen bond donors and acceptors on the pyrrolidine ring, but these would seem to be adventitious and are not likely to influence the packing significantly. Compound **6** cocrystallized with ethyl acetate, which is disordered along a channel around a  $2_1$  screw axis. In addition to one or two short contacts between the ethyl acetate and **6**, there are short intermolecular distances between a methylene C–H in the backbone and the oxygen of the amide. This is the only structure where there are any significant directional interactions that could possibly influence the turn structure. Unfortunately, compound **7**, which does not possess a hydrogen bond acceptor group, crystallized with a bound water molecule (Figure 3G) obscuring the inherent rotational preference of the fluoroamide portion of this material. Difluoroacetamide **8** crystallizes in a conformation in which one of the fluorine atoms is  $24^\circ$  removed from lying *anti* to the

amide oxygen and the other *gauche* in near perfect agreement with the theoretical model in Figure 2b.<sup>34</sup> Compound **8** also possesses strong intermolecular N–H...O interactions, forming chains that have a strong influence on the crystal packing but do not appear to influence internal rotation. Aryl difluoroamide **9** crystallizes with two distinct molecules in the unit cell, and their conformation is significantly influenced by intermolecular hydrogen bonding in the crystal, with intermolecular distances consistent with N–H...O and C–H...O interactions. The dihedral angles are again close to the maximum of the model rotational profile, opposite to what would be expected, but consistent with the potential influence of both hydrogen bonds. In addition, there is a bifurcated intermolecular C–H...F interaction from the phenyl group. In contrast to the other structures in this report, there is little evidence of any  $\pi$ – $\pi$  interaction; the only evidence of interaction between aromatic rings is a C–H... $\pi$  short contact. In general, there are no clear intermolecular interactions in the crystal that appear to be responsible for influencing the rotational states of the fluoroamide moiety for **3** and **6**.

**3. Quantum Calculations.** It is clear that the rotational profiles of the model fluoroamides are not reflected in the solid-state conformations of both mono- and difluoroamides. A more comprehensive analysis of these rotational profiles in the context of other functional groups and interactions and the ability of C–H...O H-bonds to influence conformation was undertaken.

*i. Monofluorosubstituted Systems.* Full geometry optimization of **3** at the B3LYP/6-31+G\*\* level (Figure 4A) gave a structure with  $\varphi(\text{OCCF}) = 170^\circ$ , close to the  $180^\circ$  observed in the model system; the  $10^\circ$  deviation can be attributed to the

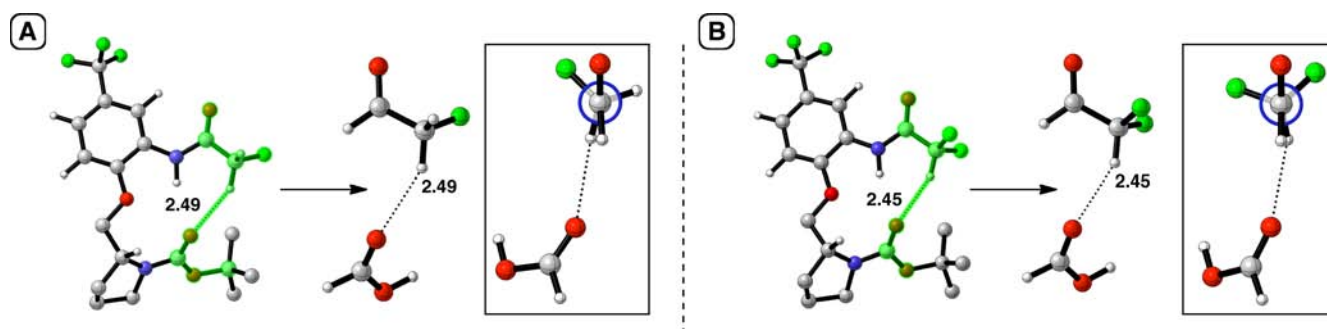


**Figure 5.** Reduction of structures of C–H···O H-bonded minima of (a) monofluoro **3** and (b) difluoro **6** substituted molecules showing smaller systems used to compute H-bond energies (some atoms omitted for clarity). Distances are in Å.

consequence of a C–H···F interaction (Figure 4A). Repulsion between the carbamate oxygen and fluorine atoms also plays a significant role, leading to a weakening of the N–H···O hydrogen bond. A rotational profile around the OC–CF bond in this molecule reveals a second minimum at a  $\varphi_{(\text{OCCF})}$  dihedral angle of  $-45^\circ$  in which a C–H···O bond occurs (length 2.49 Å), along with a shorter N–H···O interaction, consistent with amelioration of electrostatic repulsion. This structure (Figure 4B) is only 0.9 kcal mol $^{-1}$  higher than the primary minimum and an energy barrier of less than 1 kcal mol $^{-1}$  separates it from the global minimum; such small energy differences prevent unambiguous identification of the preferred conformer. Computational methods at other levels of theory lead to broadly similar results; for example, SCF computations, which include no electron correlation, change the energy difference to 0.4 kcal mol $^{-1}$ , whereas including correlation via MP2 yields a difference of 0.5 kcal mol $^{-1}$ . Reoptimization with the M06 functional for accurate treatment of noncovalent interactions verified the presence of the same two minima (within 0.4 kcal $^{-1}$  of each other and within  $7^\circ$  of the B3LYP values), and hence we are confident that these results are not an artifact of a particular theoretical method. The stability of this secondary minimum appears to be influenced by this C–H···O H-bond, since without it the structure would be as much as 6 kcal mol $^{-1}$  higher in energy than the global minimum. This idea is reinforced in the conformation of **2** (Figure 4C); there is only one minimum on the surface with a  $\varphi_{(\text{OCCF})}$  dihedral angle of  $180^\circ$ , coinciding with the theoretical model. This is consistent with the C–H···O H-bonding in **3** leading to the presence of a second minimum in the surface. However, this structure (Figure 4B) is distinct from that observed in the X-ray structure: the oxygen and fluorine atoms of the fluoroamide unit of **3** lie almost *syn* in the X-ray structure but are separated by a dihedral angle of  $45^\circ$  in the computed minimum. This anomaly can be readily explained, because rotation about the OCCF torsion (from  $45^\circ$  to  $0^\circ$ ) replaces a single C–H···O H-bond by two longer C–H···O interactions. The N–H···O hydrogen bond is also affected, contracting by 0.05 Å, consistent with strengthening of this interaction. Rotation of the computed geometry to bring it into closer coincidence with the X-ray structure raises its energy by only 0.6 kcal mol $^{-1}$ , well within the regime where intermolecular forces might exert an influence.

*ii. Difluorosubstituted Systems.* The strength of C–H···O H-bonds is directly related to the number of fluorine atoms adjacent to the donor atom, and hence we anticipated that a difluoroamide would be a stronger C–H···O H-bond donor.<sup>23</sup> This is consistent with the geometry of **6** observed by X-ray

crystal diffraction where the  $\alpha$ C–H is in close proximity to the carbamate oxygen with a C–H···O interatomic distance of 2.4 Å (C···O distance of 3.274(12)Å compared with 3.35(2)Å in **3**). To probe this, a full geometry optimization of **6** was carried out using the B3LYP/6-31+G\*\* approach leading to a structure (Figure 4D) that exhibits few minor differences to the observed structure. Remarkably, this is near the maximum of the rotational profile of the model difluoroamide (Figure 2). In order to examine this phenomenon more closely, the terminal CF<sub>2</sub>H group was rotated around the OCCF torsion, generating a series of structures that were fully optimized, tracing out a potential energy curve as a function of this dihedral angle. This demonstrated that there is a second minimum on this surface (Figure 4E) that lies slightly below the energy of the initially optimized structure (Figure 4D), by 0.1 kcal mol $^{-1}$ , and is separated from it by an energy barrier of 1.5 kcal mol $^{-1}$ . This geometry, with the fluorine distant from the carbonyl oxygen ( $\varphi_{(\text{OCCF})} = 142^\circ$ ), is similar to that expected for a difluoroamide in the absence of any intramolecular C–H···O interaction; the  $\varphi_{(\text{OCCF})}$  dihedral angle is within  $20^\circ$  of the optimized model structure (Figure 2B). In order to probe whether intramolecular interactions were influencing the intrinsic preference for OCCF *trans*-planarity, we performed a full geometry optimization of **7**, which lacks an intramolecular hydrogen bond acceptor (Figure 4F). The  $\varphi_{(\text{OCCF})}$  angle of  $158^\circ$  and the entire rotational profile are consistent with that of the model difluoroamide. In both cases, there is a shallow barrier of about 0.5 kcal mol $^{-1}$  separating two nearly equivalent minima, and a higher barrier of 4.0 kcal mol $^{-1}$  that corresponds to placement of the two fluorine atoms within  $\pm 60^\circ$  of the carbonyl oxygen atom. There is no minimum for **7** that corresponds to the observed geometry of **6**, and it is likely that this is a consequence of intramolecular interactions, including the C–H···O H-bond. The presence of the C–H···O interaction was also confirmed by natural bond order (NBO) analysis that reveals the charge transfer from the O lone pair to the C–H  $\sigma^*$  orbital, which is a fingerprint of such H-bonds.

As a control, we also examined **10**, which is not substituted with any electronegative atoms in the  $\alpha$ -position (Figure 4G).<sup>20</sup> The X-ray structure of this material shows the expected amide hydrogen-bonded turn structure, but no evidence of an intramolecular C–H···O interaction. Without polarization of the C $^\alpha$ -H, we did not expect the amide methyl group to possess a strong rotational dependence upon the OCCH dihedral angle. Calculations of this molecule show nearly free rotation about the OCCH dihedral with a very flat rotational profile, with a variation of less than 0.3 kcal/mol (Figure 4H). This is

consistent with the key role of  $\alpha$ -electronegative groups in the formation of influential C–H $\cdots$ O interactions.

These calculations refer to a molecule in the absence of any neighbors yet intermolecular interactions could perturb the equilibrium geometries, leading to differences between calculated and observed geometries. This was initially probed with self-consistent reaction field (SCRF) computations, to examine polarization of the surrounding molecules reacting to charge distribution within a central molecule. A dielectric constant of 4.0 was used, consistent with earlier estimates of its value within the confines of protein-like environments.<sup>36,37</sup> The effects were found to be quite small, affecting relative energies by only 1 kcal mol<sup>-1</sup> or less. Taking molecule 6 as an example, polarizability effects slightly favor 4D over 4E, leading to an energy difference of 1.0 kcal mol<sup>-1</sup>. In the case of the monofluorinated molecule 3, the original energy difference of 0.9 kcal mol<sup>-1</sup> between 4A and 4B is reduced and even reversed, with 4B barely more stable than 4A by 0.1 kcal mol<sup>-1</sup>. These results are consistent with examination of intermolecular interactions in the solid state.

*iii. How Strong Is the C–H $\cdots$ O Interaction?* The strength of an individual H-bond within the context of a larger system may be estimated by removing all extraneous atoms to allow computation of an unambiguous interaction energy. This approach is derived from a procedure used successfully to evaluate C–H $\cdots$ O H-bonds within the confines of a protein  $\beta$ -sheet that also contained N–H $\cdots$ O H-bonds.<sup>38</sup> Taking monofluoroamide 3 and removing all atoms except those directly related to the C–H $\cdots$ O H-bond leaves two fragments that were frozen in their precise relative orientations (Figure 5).

The energy of this complex was then compared with the energies of the isolated monomers, and the difference was taken as the interaction or C–H $\cdots$ O H-bond energy. This led to an energy of 3.0 kcal mol<sup>-1</sup>, which is relatively weak in comparison to the steep potential highlighted in the rotational profile (Figure 2A). This is consistent with the inability of this specific C–H $\cdots$ O H-bond to overcome the natural tendency of the fluorine to orient *trans*-planar to the oxygen of the amide. A similar technique was applied to the difluoroamide 6, and this led to a complexation energy of 3.5 kcal mol<sup>-1</sup>, close to the 4.0 kcal mol<sup>-1</sup> potential estimated above. This energy is comparable to the 4.0 kcal mol<sup>-1</sup> barrier associated with rotation about the OCCF torsion (Figure 2B) and hence in this case, we believe that the C–H $\cdots$ O H-interaction plays a significant role in determining conformation.

## CONCLUSION

A range of noncovalent interactions, including hydrogen bonding and electrostatic repulsion, can significantly affect the conformations of small molecules. Nominally weak hydrogen bonds such as the C–H $\cdots$ O interaction are often overpowered by other effects, but their influence can be augmented by incorporation of electronegative substituents adjacent to the donor atom. In this study, we have demonstrated that such activation can influence the intrinsic *trans*-planar preference of  $\alpha$ -fluoroamides through a combination of electrostatic and hydrogen bonding effects. Violation of the preference for monofluoro- and difluoroamides to place the amide oxygen and  $\alpha$ -fluorine atoms as far away from each other as possible costs approximately 6 and 4 kcal mol<sup>-1</sup>, respectively, but this may be recouped to some extent by the formation of intramolecular N–H $\cdots$ O and C–H $\cdots$ O hydrogen bonds. In the case of the fluoroamides 3 and 6, electrostatic repulsion between the

carbamate oxygen and the fluorine atoms of the fluoroamide favor a conformation in which C–H $\cdots$ O interactions can play a significant role. This oxygen–fluorine repulsion alone does not account for the observed rotameric preference of the fluoroamides, and calculations of model systems suggest the attractive energy of the C–H $\cdots$ O interaction to be 3.0 and 3.5 kcal mol<sup>-1</sup>, respectively, for the mono- and difluoroamide systems. In the case of monofluoroamide 3, a C–H $\cdots$ O hydrogen bonded conformation represents a minimum in the rotational profile, but this C–H $\cdots$ O H-bond is relatively weak, and the natural rotational profile of the fluoroamide is steep enough that this is not a determinant of conformation. In the case of the difluorinated system 6, however, the C–H $\cdots$ O H-bond is strong enough relative to the rotational potential to overcome the *trans*-planar effect, and hence this constitutes a rare system where, in combination with the electrostatic effects, the C–H $\cdots$ O H-bond can be considered a determinant of overall conformation. These complexation energies are consistent with estimations for the isolated C–H $\cdots$ O interaction of CH<sub>2</sub>F<sub>2</sub> or glycine with water (both of which are approximately 2.5 kcal mol<sup>-1</sup>).<sup>11</sup> The extra electronegative atom increases the complexation energy by approximately 0.5–1 kcal mol<sup>-1</sup>;<sup>23</sup> this is in contrast to an unsubstituted system 10, which has essentially free rotation about the OCCF dihedral. In comparison to calculation of the strength of a C–H $\cdots$ O interaction in a membrane protein,<sup>14</sup> these energies are larger and may reflect the relative ease with which a small and relatively flexible system such as the turn structures described herein can attain optimum geometrical and distance parameters. The specific materials examined in this study demonstrate that a single C–H $\cdots$ O interaction (rather than an ensemble, as would be expected in a larger system) can be shown to stabilize an otherwise unfavorable arrangement of atoms. This testifies to the potential influence of the C–H $\cdots$ O hydrogen bond, and extrapolation of this tenet to other  $\alpha$ -electronegative substituted systems (such as those in proteins, in which a complex manifold of interactions are potentially important) is consistent with the assignment of C–H $\cdots$ O hydrogen bonds as a significant contributor to overall conformation in both model and natural systems.

## METHODS

For full experimental details and X-ray and spectral data, see Supporting Information. Low-temperature, single crystal diffraction data were collected on I19 (EH1) at the Diamond Light Source, using a Nonius Kappa CCD diffractometer<sup>39</sup> or an Oxford Diffraction Supernova and were solved using SIR92<sup>40</sup> or SuperFlip.<sup>41</sup> Refinement was carried out within the CRYSTALS suite,<sup>42,43</sup> and hydrogen atoms were refined prior to inclusion in the refinement using a riding model<sup>44</sup> or using ShelXL<sup>45</sup> where hydrogen atoms were located geometrically and repositioned after each cycle. Dihedral angles and short contacts were calculated using PLATON.<sup>46</sup> Calculations were carried out via the GAUSSIAN03 code.<sup>47</sup> The 6-31+G\*\* double- $\zeta$  quality basis set contains polarization functions on all atoms, augmented by diffuse functions on heavy atoms; the larger and more flexible aug-cc-pVDZ basis set was also used. The B3LYP variant of density functional theory (DFT)<sup>48,49</sup> was used because it has had good success in the past with related molecules.<sup>50–55</sup> Complementary calculations were carried out with M06,<sup>56</sup> a recently developed functional with a focus on noncovalent interactions such as H-bonds. Second-order Møller–Plesset (MP2) was used as a more complete means of including electron correlation. The self-consistent reaction field (SCRF) approach<sup>57–59</sup> was applied to study the effects of a surrounding polarizable medium, with a dielectric constant  $\epsilon$ . The polarizable continuum method (PCM)<sup>60–62</sup> embeds the solute in a

cavity that reproduces the shape of the molecule by a series of overlapping spheres. The particular variant of this method used here is the conductor polarized continuum model (CPCM)<sup>63</sup> wherein the apparent charges distributed on the cavity surface are such that the total electrostatic potential cancels on the surface. Recent calculations<sup>64</sup> have shown that the CPCM variant provides results that are in good agreement with other approaches, notably PCM and SCIPCM, in treating the C–H···O interaction as well as conventional H-bonds.

## ■ ASSOCIATED CONTENT

### 📄 Supporting Information

Full synthetic details, <sup>1</sup>H and <sup>13</sup>C NMR spectra, and crystallographic data in cif format. This material is available free of charge via the Internet at <http://pubs.acs.org>. The crystal structure data of **2**, **3**, **4**, **5**, **6**, **7**, and **9** have been deposited in the Cambridge Crystallographic Data Centre (CCDC reference numbers 886717, 886718, 886719, 886720, 886721, 886722, and 886724, respectively).

## ■ AUTHOR INFORMATION

### Corresponding Author

[martin.smith@chem.ox.ac.uk](mailto:martin.smith@chem.ox.ac.uk); [steve.scheiner@usu.edu](mailto:steve.scheiner@usu.edu)

### Notes

The authors declare no competing financial interest.

## ■ ACKNOWLEDGMENTS

We are grateful for support from the Royal Society (for a URF to M.D.S.), the EPSRC and Organon (for a CASE award to C.R.J.), the EU (for a Marie Curie award to P.K.B.), and the EPSRC and NSF (to S.S. and M.D.S.). S.S. acknowledges support from the NSF, Grant CHE-1026826. We gratefully acknowledge the Diamond Light Source for an award of instrument time on I19 (MT1858) and the instrument scientists (Dr. David R. Allan and Dr. Kirsten E. Christensen) for support. The assistance of Dr. John Davies (University of Cambridge) for X-ray analysis is gratefully acknowledged. The European Research Council has provided financial support under the European Community's Seventh Framework Programme (FP7/2007-2013)/ERC Grant Agreement No. 259056.

## ■ REFERENCES

- (1) Senes, A.; Ubarretxena-Belandia, I.; Engelman, D. M. *Proc. Natl. Acad. Sci. U.S.A.* **2001**, *98*, 9056–9061.
- (2) Derewenda, Z. S.; Derewenda, U.; Kobos, P. M. *J. Mol. Biol.* **1994**, *241*, 83–93.
- (3) Derewenda, Z. S.; Lee, L.; Derewenda, U. *J. Mol. Biol.* **1995**, *252*, 248–262.
- (4) Bella, J.; Berman, H. M. *J. Mol. Biol.* **1996**, *264*, 734–742.
- (5) Fabiola, G. F.; Krishnaswamy, S.; Nagarajan, V.; Pattabhi, V. *Acta Crystallogr.* **1997**, *D53*, 316–320.
- (6) Taylor, R.; Kennard, O. *J. Am. Chem. Soc.* **1982**, *104*, 5063–5070.
- (7) Nagawa, Y.; Yamagaki, T.; Nakanishi, H.; Nakagawa, M.; Takahiro, T. *Tetrahedron Lett.* **1998**, *39*, 1393–1396.
- (8) Dunitz, J. D.; Gavezzotti, A. *Angew. Chem., Int. Ed.* **2005**, *44*, 1766–1787.
- (9) Park, H.; Yoon, J.; Seok, C. *J. Phys. Chem. B.* **2008**, *112*, 1041–1048.
- (10) Vargas, R.; Garza, J.; Dixon, D. A.; Hay, B. P. *J. Am. Chem. Soc.* **2000**, *122*, 4750–4755.
- (11) Scheiner, S.; Kar, T.; Gu, Y. *J. Biol. Chem.* **2001**, *276*, 9832–9837.
- (12) Castellano, R. K. *Curr. Org. Chem.* **2004**, *8*, 845–865.

- (13) Yohannan, S.; Faham, S.; Yang, D.; Grosfeld, D.; Chamberlain, A. K.; Bowie, J. U. *J. Am. Chem. Soc.* **2004**, *126*, 2284–2285.
- (14) Mottamalm, M.; Lazaridis, T. *Biochemistry* **2005**, *44*, 1607–1613.
- (15) Seiler, P.; Weisman, R.; Glendening, E. D.; Weinhold, F.; Johnson, V. B.; Dunitz, J. D. *Angew. Chem., Int. Ed. Engl.* **1987**, *26*, 1175–1177.
- (16) Seiler, P.; Dunitz, J. D. *Helv. Chim. Acta* **1989**, *72*, 1125–1135.
- (17) Paton, R. S.; Goodman, J. G. *Org. Lett.* **2006**, *8*, 4299–4302.
- (18) Corey, E. J.; Rohde, J. J.; Fischer, A.; Azimioara, M. D. *Tetrahedron Lett.* **1997**, *38*, 33–36.
- (19) Scheiner, S. *Curr. Org. Chem.* **2010**, *14*, 106–128.
- (20) Jones, C. R.; Qureshi, M. K. N.; Truscott, F. R.; Hsu, S.-T. D.; Morrison, A. J.; Smith, M. D. *Angew. Chem., Int. Ed.* **2008**, *47*, 7099–7102.
- (21) Jones, C. R.; Pantos, G. D.; Morrison, A. J.; Smith, M. D. *Angew. Chem., Int. Ed.* **2009**, *48*, 7391–7394.
- (22) O'Hagan, D. *Chem. Soc. Rev.* **2008**, *37*, 308–319.
- (23) Gu, Y.; Kar, T.; Scheiner, S. *J. Am. Chem. Soc.* **1999**, *121*, 9411–9422.
- (24) Banks, J. W.; Batsanov, A. S.; Howard, J. A. K.; O'Hagan, D.; Rzepa, H. S.; Martin-Santamaria, S. *J. Chem. Soc., Perkin Trans. II* **1999**, 2409–2411.
- (25) Tormena, C. F.; Amadeu, N. S.; Rittner, R.; Abraham, R. J. *J. Chem. Soc., Perkin Trans. II* **2002**, 773–778.
- (26) Briggs, C. R. S.; O'Hagan, D.; Howard, J. A. K.; Yufit, D. S. *J. Fluorine Chem.* **2003**, *119*, 9–13.
- (27) Hunter, L. *Beilstein J. Org. Chem.* **2010**, *6*, 38.
- (28) Steiner, T. *J. Phys. Chem. A* **2000**, *104*, 433–435.
- (29) Mathad, R. I.; Gessier, F.; Seebach, D.; Jaun, B. *Helv. Chim. Acta* **2003**, *88*, 266–280.
- (30) Mathad, R. I.; Jaun, B.; Flögel, O.; Gardiner, J.; Löweneck, M.; Codée, J. D. C.; Seeberger, P. H.; Seebach, D.; Edmonds, M. K.; Graichen, F. H. M.; Abell, A. D. *Helv. Chim. Acta* **2007**, *90*, 2251–2273.
- (31) Gattin, Z.; van Gunsteren, W. F. *J. Phys. Chem. B* **2009**, *113*, 8695–8703.
- (32) Hunter, L.; Jolliffe, K. A.; Jordan, M. J. T.; Jensen, P.; Macquart, R. B. *Chem.—Eur. J.* **2011**, *17*, 2340–2343.
- (33) Hughes, D. O.; Small, R. W. H. *Acta Crystallogr.* **1962**, *15*, 933–940.
- (34) Hughes, D. O.; Small, R. W. H. *Acta Crystallogr.* **1972**, *B28*, 2520–2524.
- (35) Jaun, B.; Seebach, D.; Mathad, R. I. *Helv. Chim. Acta* **2011**, *94*, 355–361.
- (36) Sharp, K. A.; Honig, B. *Annu. Rev. Biophys. Biophys. Chem.* **1990**, *19*, 301–335.
- (37) Dwyer, J. J.; Gittis, A. G.; Karp, D. A.; Lattman, E. E.; Spencer, D. S.; Stites, W. E.; Garcia-Moreno, B. *Biophys. J.* **2000**, *79*, 1610–1620.
- (38) Scheiner, S. *J. Phys. Chem. B* **2006**, *110*, 18670–18679.
- (39) Otwinowski, Z.; Minor, W. *Methods Enzymol.* **1997**, *276*, 307–326.
- (40) Altomare, A.; Cascarano, G.; Giacovazzo, C.; Guagliardi, A.; Burla, M. C.; Polidori, G.; Camalli, M. *J. Appl. Crystallogr.* **1994**, *27*, 435.
- (41) Palatinus, L.; Chapuis, G. *J. Appl. Crystallogr.* **1997**, *40*, 786–790.
- (42) Betteridge, P. W.; Carruthers, J. R.; Cooper, R. I.; Prout, K.; Watkin, D. J. *J. Appl. Crystallogr.* **2003**, *36*, 1487.
- (43) Thompson, A. L.; Watkin, D. J. *J. Appl. Crystallogr.* **2011**, *44*, 1017–1022.
- (44) Cooper, R. I.; Thompson, A. L.; Watkin, D. J. *J. Appl. Crystallogr.* **2010**, *43*, 1100–1107.
- (45) Sheldrick, G. M. *Acta Crystallogr.* **2008**, *A64*, 112–122.
- (46) Spek, A. *J. Appl. Crystallogr.* **2003**, *36*, 7–13.
- (47) Frisch, M. J.; Trucks, G. W.; Schlegel, H. B.; Scuseria, G. E.; Robb, M. A.; Cheeseman, J. R.; Montgomery, J. A., Jr.; Vreven, T.; Kudin, K. N.; Burant, J. C.; Millam, J. M.; Iyengar, S. S.; Tomasi, J.;

Barone, V.; Mennucci, B.; Cossi, M.; Scalmani, G.; Rega, N.; Petersson, G. A.; Nakatsuji, H.; Hada, M.; Ehara, M.; Toyota, K.; Fukuda, R.; Hasegawa, J.; Ishida, M.; Nakajima, T.; Honda, Y.; Kitao, O.; Nakai, H.; Klene, M.; Li, X.; Knox, J. E.; Hratchian, H. P.; Cross, J. B.; Bakken, V.; Adamo, C.; Jaramillo, J.; Gomperts, R.; Stratmann, R. E.; Yazyev, O.; Austin, A. J.; Cammi, R.; Pomelli, C.; Ochterski, J. W.; Ayala, P. Y.; Morokuma, K.; Voth, G. A.; Salvador, P.; Dannenberg, J. J.; Zakrzewski, V. G.; Dapprich, S.; Daniels, A. D.; Strain, M. C.; Farkas, O.; Malick, D. K.; Rabuck, A. D.; Raghavachari, K.; Foresman, J. B.; Ortiz, J. V.; Cui, Q.; Baboul, A. G.; Clifford, S.; Cioslowski, J.; Stefanov, B. B.; Liu, G.; Liashenko, A.; Piskorz, P.; Komaromi, I.; Martin, R. L.; Fox, D. J.; Keith, T.; Al-Laham, M. A.; Peng, C. Y.; Nanayakkara, A.; Challacombe, M.; Gill, P. M. W.; Johnson, B.; Chen, W.; Wong, M. W.; Gonzalez, C.; Pople, J. A. *Gaussian 03*, revision D.01; Gaussian, Inc.: Wallingford, CT, 2003.

(48) Becke, A. D. *J. Chem. Phys.* **1993**, *98*, 5648–5652.

(49) Lee, C.; Yang, W.; Parr, R. G. *Phys. Rev. B* **1988**, *37*, 785–789.

(50) Rablen, P. R.; Lockman, J. W.; Jorgensen, W. L. *J. Phys. Chem. A* **1998**, *102*, 3782–3797.

(51) Rao, L.; Ke, H.; Fu, G.; Xu, X.; Yan, Y. *J. Chem. Theory Comput.* **2009**, *5*, 86–96.

(52) Esrafil, M. D.; Hadipour, N. L. *Mol. Phys.* **2011**, *109*, 2451–2460.

(53) Zvereva, E. E.; Shagidullin, A. R.; Katsyuba, S. A. *J. Phys. Chem. A* **2011**, *115*, 63–69.

(54) Plumley, J. A.; Dannenberg, J. J. *J. Comput. Chem.* **2011**, *32*, 1519–1527.

(55) Bühl, M.; Kilian, P.; Woollins, J. D. *ChemPhysChem* **2011**, *12*, 2405–2408.

(56) Zhao, Y.; Truhlar, D. G. *Theor. Chem. Acc.* **2008**, *120*, 215–241.

(57) Onsager, L. *J. Am. Chem. Soc.* **1936**, *58*, 1486–1493.

(58) Wong, M. W.; Frisch, M. J.; Wiberg, K. B. *J. Am. Chem. Soc.* **1991**, *113*, 4776–4782.

(59) Wong, M. W.; Wiberg, K. B.; Frisch, M. J. *J. Chem. Phys.* **1991**, *95*, 8991–8998.

(60) Miertus, S.; Scrocco, E.; Tomasi, J. *J. Chem. Phys.* **1981**, *55*, 117–129.

(61) Miertus, S.; Tomasi, J. *J. Chem. Phys.* **1982**, *65*, 239–245.

(62) Mennucci, B.; Tomasi, J. *J. Chem. Phys.* **1997**, *106*, 5151–5198.

(63) Barone, V.; Cossi, M. *J. Phys. Chem. A* **1998**, *102*, 1995–2001.

(64) Scheiner, S.; Kar, T. *J. Phys. Chem. B* **2005**, *109*, 3681–3689.